

# Discontinuous Grain Boundaries of Forged René 41

---

**Steven Crump**

**Advisor: Prof. Blair London**

**Industry Sponsor: Carlton Forge Works**

# Approval Page

Project Title: Discontinuous Grain Boundaries of Forged René 41

Author: Steven Crump

Date Submitted: 6/1/2012

CAL POLY STATE UNIVERSITY

Materials Engineering Department

Since this project is a result of a class assignment, it has been graded and accepted as fulfillment of the course requirements. Acceptance does not imply technical accuracy or reliability. Any use of the information in this report, including numerical data, is done at the risk of the user. These risks may include catastrophic failure of the device or infringement of patent or copyright laws. The students, faculty, and staff of Cal Poly State University, San Luis Obispo cannot be held liable for any misuse of the project.

Prof. Blair London

---

Faculty Advisor

Signature

Prof. Trevor Harding

---

Department Chair

Signature

## Abstract

Forged components must pass a grain size specification (grain size, distribution) for acceptance in an application. The varying amounts of plastic deformation during forging can lead to abnormally large recrystallized grain sizes in certain regions of the part, which will not pass specification. The question exists whether these abnormally coarse grains are truly comprised of poly crystalline fine grains with grain boundaries resistant to etching techniques. To investigate this abnormal grain size effect, a cross section of a forged René 41 nickel-based superalloy aircraft engine ring was cut and sectioned into six segments. Those segments were then prepared for microstructural analysis using a 95% HCl and 5% H<sub>2</sub>O<sub>2</sub> etch typical of metallographic testing companies. The results indicated an apparent segregation of the grains with multiple regions showing a few abnormally large grains surrounded by much smaller ones. A fine grain size dominated some samples (ASTM grain size 5 to 7), these would pass specification. Other regions showed intermittent large grains (ASTM grain size 1 to 2). The presence of annealing twins within the large grains proved that these larger grains were single grains, but their true size is masked by discontinuous boundaries throughout. The abnormally large grains followed some flow pattern suggesting their manifestation may be a function of how much strain was applied to that section of the alloy during forging. Scanning electron microscopy (SEM) in conjunction with electron backscatter diffraction (EBSD), determined the orientation and size of each grain on a map and identified grains independently of etching grain boundaries. As a result, the discontinuous grain boundaries in question were determined to be low angle grain boundaries that were resistant to chemical attack by the etchant.

Key Words: Materials Engineering, Superalloys, René 41, grain boundaries, Electron Backscatter Diffraction, EBSD, low angle grain boundaries

## Table of Contents

Abstract .....	2
List of Figures .....	4
Introduction .....	6
Superalloys in Industry.....	6
Realistic Constraints <sup>(4)</sup> .....	7
Manufacturability Factors.....	7
Economic Consequences.....	8
Rene 41 Microstructure .....	8
Processing René 41 .....	9
Discontinuous Grain Boundaries.....	10
Scanning Electron Microscopy .....	14
Experimental Procedure .....	16
Metallographic Preparation.....	16
Metallographic Grain Size Measurement .....	17
Measuring Fine Grains .....	17
Estimation of Large Grain Sizes.....	18
SEM-EBSD Preparation.....	19
Results.....	20
Fine Grain Sizes .....	20
Coarse Grain Sizes.....	21
Optical Verification of Discontinuous Grains.....	22
SEM-EBSD.....	23
Image Quality Map.....	23
Inverse Pole Figure.....	24
Discussion.....	25
Topological Duplex Grain .....	25
Correlation between Discontinuous and Low Angle Grain Boundaries.....	25
Recommendation for Further Study .....	26
Conclusions .....	26
References .....	27
Acknowledgements.....	29



## List of Figures

Figure 1: A cut away diagram of the Pratt & Whitney engine used to power the F-16 jet fighter. The blue colored sections indicate a cooler relative temperature when compared to the red and orange areas. <sup>(3)</sup>	6
Figure 2: A diagram illustrating the ring rolling process from the upset punch to the rolling of the seamless ring. <sup>(8)</sup>	9
Figure 3: Microstructure of René 41 after forging. Note the grain boundaries in amongst in the coarser grain that do not form a closed loop.	10
Figure 4: Strings of precipitates form incoherent boundaries that may explain why some boundaries look continuous while others do not.	12
Figure 5: A diagram of two simple cubic cell lattices twisted about the $\langle 100 \rangle$ direction at $53.1^\circ$ . <sup>(11)</sup> Large open circles represent possible locations for coincident sites between lattices.	13
Figure 6: A Schematic showing the incident electron beam striking the lattice and the resulting electrons scattering. <sup>(14)</sup>	14
Figure 7: An example of Kikuchi bands formed from secondary electrons scattering off of a nickel sample. <sup>(14)</sup> A computer generated crystal lattice is superimposed with planes highlighted to show orientation relative to the Kikuchi bands.	15
Figure 8: An example a grain size and direction map using inverse pole figures. <sup>(14)</sup>	15
Figure 9: A figure demonstrating how orientation is captured by an inverse pole figure map with color coding. <sup>(14)</sup>	15
Figure 10: A schematic of the cross section detailing where samples originated from.	16
Figure 11: An example of how grain size was measured using a computer overlay of the diagonal measuring tool. Each of the blue marks indicates a manually marked grain boundary intersection. ....	17
Figure 12: A micrograph describing the technique used for measuring the largest grain (ALA) of a sample.	18

Figure 13: An excerpt from ASTM standard 1181-02 comparison chart of relative percentages of duplex grain size. <sup>(17)</sup> .....	19
Figure 16: Sample A showing a small band of fine grains in amongst much coarser grains. ....	20
Figure 15: A box plot of average fine grain sizes in samples D, E, J, and M with a pooled standard deviation of 0.357. ....	20
Figure 17: A purposefully over etched sample of a typical large grain seen with twinning boundaries running across.....	21
Figure 18: Distribution of large grains across the cross section. ....	21
Figure 19: A micrograph of a discontinuous grain taken at 500x where there is a clear distinction between twinning boundaries, precipitates, and discontinuous grain boundaries .....	22
Figure 21: An overlay of possible low angle boundaries over the original image quality map of figure 20. Red and Green lines illustrate low angle grain boundaries; however green lines are lower angle than red. ....	23
Figure 20: An image quality map, produced by EBSD, shows the majority of the area being consumed by large grains.....	23
Figure 23: An inverse pole figure relating a specific color to a particular crystallographic orientation.....	24
Figure 22: A color map type describing how the real world vectors [001], [101], and [111] correlate to the colors red, green, and blue respectively. ....	24

## Introduction

### Superalloys in Industry

The superalloy industry provides a unique service to many other industries by providing alloys that maintain superior material properties at high temperatures. Applications range from jet engines on aircraft such as the Boeing 787 Dreamliner to land based components within a nuclear power plant like Diablo Canyon power plant in San Luis Obispo County, CA, operated by Pacific Gas and Electric. Nickel, cobalt, and nickel-iron alloys are common types of superalloys due to their retention of properties in either high temperature or corrosive conditions<sup>(1)</sup>. Of the nickel based alloys, René 41 is widely used in gas turbine engines because it is one of the strongest high temperature alloys on the market. This is particularly useful when temperatures in a combustion chamber of a jet engine can regularly reach above 1470°F<sup>(1)</sup>. Common components using René 41 include tracks, turbine casings, nozzle diaphragms, and combustion liners (Figure 1)<sup>(2)</sup>. Carlton Forge Works (Paramount CA) produces forged nickel based alloys such as René 41 for the specific application of Jet Engines.<sup>(3)</sup>

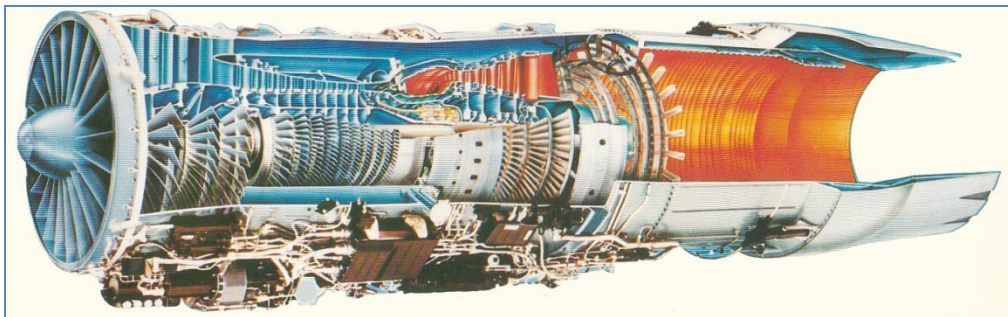


Figure 1: A cut away diagram of the Pratt & Whitney engine used to power the F-16 jet fighter. The blue colored sections indicate a cooler relative temperature when compared to the red and orange areas.<sup>(3)</sup>

## Realistic Constraints <sup>(4)</sup>

Superalloys are critical to a number of industries that require materials that retain properties at high temperatures, but for this project are more specific to aerospace applications. Development of this special class of alloy first emerged shortly after World War II when interest in high temperature jet engines began to emerge. <sup>(5)</sup> The importance of superalloys can be put into perspective by the amount used in a typical engine. Over 50% by weight of a turbine engine is made of superalloys. <sup>(5)</sup> Global civilian aviation is a cornerstone in our modern society allowing people and products to travel safely, swiftly, and efficiently <sup>(1)</sup>. Some realistic constraints like manufacturability and economic factors can be addressed by this project.

## Manufacturability Factors

My project specifically applies to the manufacturability of René 41 with respect to grain formation but has broader implications. Some René 41 forged parts exhibit a discontinuous grain structure however this microstructure is found in other superalloys as well. Discontinuous grains are currently not well understood so parts that exhibit these grains are unsuitable for the customer. By characterizing the microstructure, a better understanding of the connections between processing and the resulting grain structure can be established. A quantitative statistical analysis could also be done to establish the material properties of the unique grains. Knowing the material properties of these discontinuous grains can help forging companies like Carlton Forge Works decide whether these parts meet adequate standards even though they have unusual grain structures. Also, knowing the circumstances under which these grains form can help engineers modify forging processes to avoid such grain structures if these grains are determined to be sub-standard.

## Economic Consequences

As mentioned above, characterization of the grain structure can increase the overall manufacturability of these nickel based superalloys. By increasing the number of components that are accepted, the costs associated with forging will drop and result in less waste in either reprocessing or scrapping the parts. This works to improve the efficiency of Carlton Forge Works so that they are more competitive in the international market. Currently, the United States boasts one of the most competitive aerospace industries with a positive trade balance of \$44.1 billion and is the largest trade surplus of any US industry.<sup>(6)</sup>

## Rene 41 Microstructure

The first step in the characterization process of the discontinuous grains is identifying definitively what grain structure is present.<sup>(7)</sup> While the scope of the project will not solve the problem of characterizing the material properties of discontinuous grains, it is a step in the right direction in determining what kinds of boundaries they are. René 41 owes its strength to both precipitation hardening and solid solution strengthening mechanisms.<sup>(2)</sup> During the aging process, a coherent ordered face centered cubic gamma prime phase ( $\text{Al}_3\text{Ni}$ ) precipitates at the grain boundaries which act as the primary strengthening mechanism. Provided that the alloy is peak aged, the boundary between the gamma phase and particles of the gamma prime phase provide a substantial barrier to dislocation movement.<sup>(1)</sup> Molybdenum and cobalt are the primary alloying elements used for solid solution strengthening because they substitute for nickel atoms in the gamma phase FCC lattice. The stress induced by these alloying elements act to impede dislocation movement. Cobalt also reduces the solubility of aluminum and titanium in the gamma matrix, thus increasing gamma-prime precipitation.<sup>(2)</sup>

## Processing René 41

Carlton Forge Works, based in Paramount, CA, specializes in forging rings of various sizes up to 180 inches in diameter. The forging process starts with a mill annealed ingot with a given composition and grain size. The annealing temperature is typically 1975°F and followed by a water quench to below 1200°F within 3 to 5 seconds to achieve softness and formability during forging operations.<sup>(2)</sup> The annealed ingots are hot worked by upsetting and punching the ingot into a ring shape by shortening the length of the ingot and expanding the radius while inserting a hole at the center. They are then rolled and closed die forged to shape<sup>(8)</sup> (Figure 2). Throughout this process, the forging is kept at an elevated temperature range to avoid unwanted phases from forming at the upper temperature range and rapid work hardening at the lower range. At this point, the grains are highly deformed and are not the correct structure, therefore the ring is heat treated to achieve an adequate microstructure.

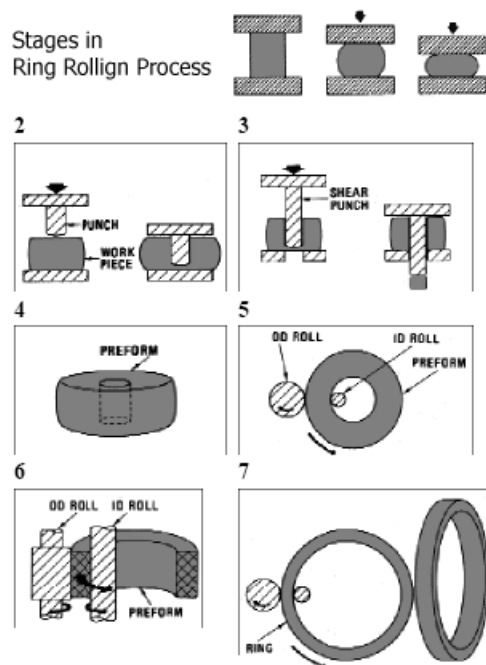


Figure 2: A diagram illustrating the ring rolling process from the upset punch to the rolling of the seamless ring.<sup>(8)</sup>

Following the hot working process, the ring is solution treated between 1950°F and 2050°F and air cooled produce a recrystallized structure. The alloy is then aged between 1400°F and 1650°F to allow gamma prime precipitates to form to further strengthen the material by providing more impediments to dislocation movement. High solution treating and aging temperatures produce better stress-rupture properties while lower heat treating and aging temperatures increase short term tensile strength.<sup>(2)</sup>

## Discontinuous Grain Boundaries

Although René 41 provides great strength and high temperature mechanical properties, it also occasionally suffers from a phenomenon of developing grain boundaries that seem to lead to nowhere (Figure 3). This phenomenon is not exclusive to René 41 but also occurs in other nickel alloys like IN718 and has been an issue with the forging industry for a long time.<sup>(9)</sup>

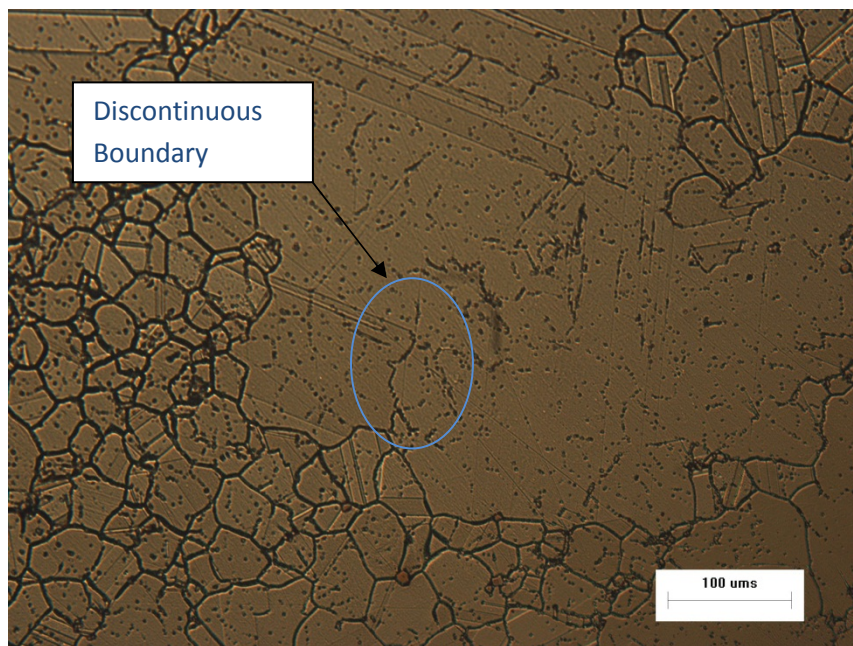


Figure 3: Microstructure of René 41 after forging. Note the grain boundaries in amongst in the coarser grain that do not form a closed loop.

### *Abnormal Grain Growth*

Abnormal grain growth during hot working or heat treatment can cause grains to rapidly increase in size.

The two principal mechanisms of abnormal grain growth in nickel alloys include absorption of

surrounding grains due to grain boundary migration, and formation of new grains during

recrystallization and subsequent grain boundary migration.<sup>(10)</sup> Both mechanisms involve strain induced

grain boundary migration where grains with higher strain are absorbed by grains with lower strain. The

difference in energy between grains can be attributed to non-uniform metal flow during hot working.

Non-uniform metal flow or thermal stresses during quenching can result in critical deformation. Critical

deformation is the minimum requirement of strain applied to an alloy so that there is enough stored

energy to promote grain growth during recrystallization. Critical deformation has been directly linked to

abnormal grain growth in nickel based alloys. In most cases, a reduction of 5% is adequate to ensure

that the part does not undergo abnormal grain growth.<sup>(10)</sup>

The presence of abnormally coarse grains has been linked to poor properties in high temperature nickel

based alloys like René 41.<sup>(10)</sup> Typically, a part with abnormal grains would have low unsatisfactory

material properties like ductility. A low ductility would be grounds for part rejection. However, the

samples provided by Carlton Forge Works have been tested by Dixon Testing Company (South Gate, CA)

and have passed mechanical testing requirements. Therefore, abnormal grains are not likely to be the

culprit.



### *Annealing Precipitates*

A second possibility is that the discontinuous grain boundaries are just a line of precipitates. Precipitates initially formed at grain boundaries in the annealed structure. However during the solution heat treatment, some of the precipitates at these grain boundaries do not fall back into solution because they are precipitates that maintain structure at high temperatures. As a result, these precipitates that were at grain boundaries do not move when new grains are formed during recrystallization. Thus, a ghost structure of the former grain boundaries is outlined by the precipitates (Figure 4). This could easily be mistaken for possible intermittent grain boundaries for an untrained metallurgist.<sup>(9)</sup>

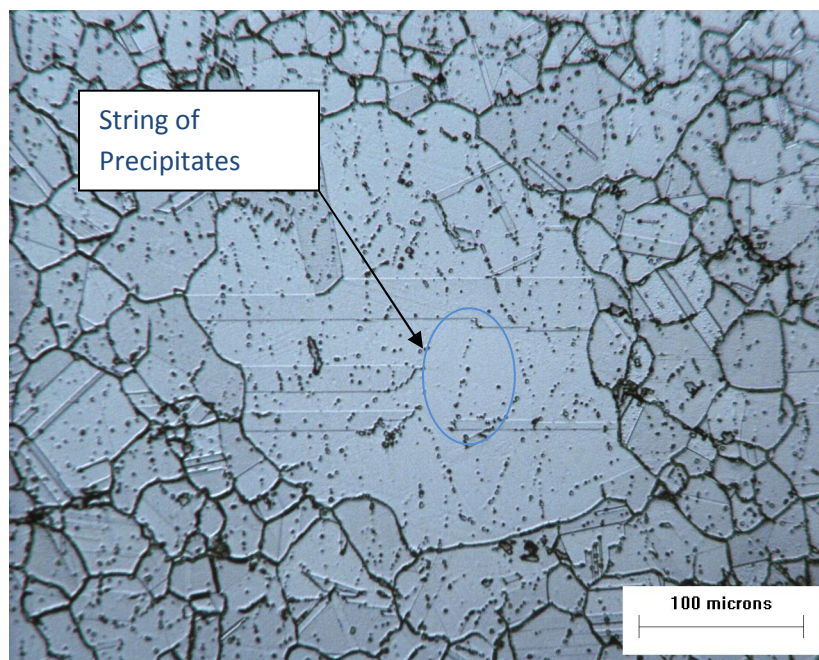
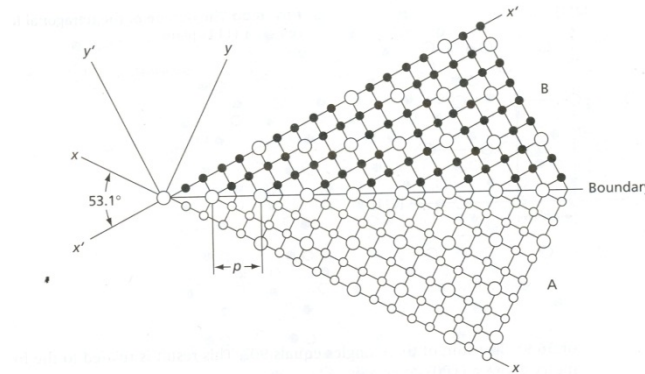


Figure 4: Strings of precipitates form incoherent boundaries that may explain why some boundaries look continuous while others do not.

### *Special Grain Boundaries*

A third explanation is the existence of special grain boundaries. These grain boundaries can be characterized as occurring between coincident-site lattices (CSL) where the lattice of one grain lines up near perfectly with the lattice of another grain and shares several sites between grains (Figure 5).<sup>(11)</sup>



**Figure 5: A diagram of two simple cubic cell lattices twisted about the  $\langle 100 \rangle$  direction at  $53.1^\circ$ .<sup>(11)</sup> Large open circles represent possible locations for coincident sites between lattices.**

Grain boundaries may be modeled as twisted, where the neighboring lattice is rotated about an axis that is parallel to the normal of the grain boundary, tilted, where the neighboring lattice is rotated about an axis that is perpendicular to the normal of the grain boundary, or a combination of both.<sup>(7)</sup> A coincident site is an atom shared by both lattices. The density count,  $\Sigma$ , is the reciprocal number of the fraction of coincident sites in a boundary. Therefore, if one third of the lattice sites match between grains, then the  $\Sigma$  value would be  $\Sigma 3$ .<sup>(11)</sup> A grain boundary angle of  $15^\circ$  or less is considered to be a low angle grain boundary with a density count of  $\Sigma 1$ . These special grain boundaries have been found to have relatively low surface energy when compared to higher angle boundaries. Lower surface energy reduces the likelihood of chemical attack because it is less favorable than higher energy surfaces that are nearby. Consequently, metallographic etchants would have a reduced effect on special grain boundaries making them harder to view under an optical microscope.<sup>(12)</sup>

Also, these special grain boundaries have also been found to increase resistance to intergranular cracking by creep and stress corrosion in nickel based superalloy IN718.<sup>(13)</sup> In this instance however, the low angle boundaries were induced through cold working and annealing, not hot working like in the case of forged René 41 rings.

## Scanning Electron Microscopy

Typical etching techniques have proven to be ineffective at clearly delineating these possible special grain boundaries described by Carlton Forge Works, so alternative methods must be used to characterize them. Utilizing scanning electron microscopy (SEM) in conjunction with electron backscatter diffraction (EBSD) offered insight into the problem without relying on optical analysis.

EBSD works by sending a focused electron beam at the sample at an angle of approximately 70° from the normal which scatters some secondary electrons (Figure 6).<sup>(14)</sup> Some of the scattered electrons are incident on the atomic planes at angles that satisfy the Bragg equation (Equation 1).

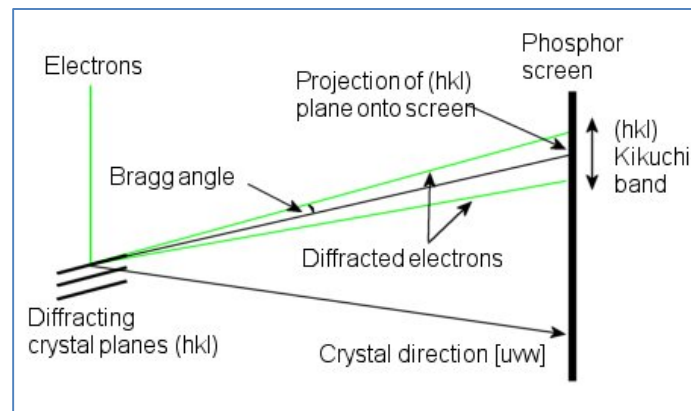


Figure 6: A Schematic showing the incident electron beam striking the lattice and the resulting electrons scattering.<sup>(14)</sup>

$$n\lambda = 2d\sin(\theta) \quad (1)$$

Where;  $n$  is an integer,  $\lambda$  is the wavelength of an electron,  $d$  is the spacing of the diffracting lattice, and  $\theta$  is the angle of incidence of the striking electrons.<sup>(20)</sup>

The bands formed from the resulting reflection are called Kikuchi bands (Figure 7).<sup>(14)</sup> The center of each Kikuchi band corresponds to a projection of a diffracting plane. Then a program can compile these orientations into a color coded map showing (Figure 8). This is done by calculating the direction of each lattice and creating an inverse pole figure. An inverse pole figure shows how a selected direction in the sample reference frame, a specific color, is distributed in the reference frame of the crystal (Figure 9).

<sup>(14)</sup> The resulting image can effectively characterize grain boundaries by knowing the angle of orientation between each grain. This makes EBSD a very effective tool in understanding the orientation of grains in a poly crystalline material like René 41.

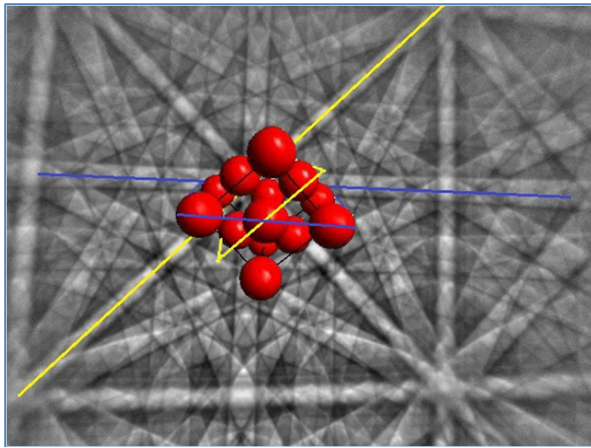


Figure 7: An example of Kikuchi bands formed from secondary electrons scattering off of a nickel sample.<sup>(14)</sup> A computer generated crystal lattice is superimposed with planes highlighted to show orientation relative to the Kikuchi bands.

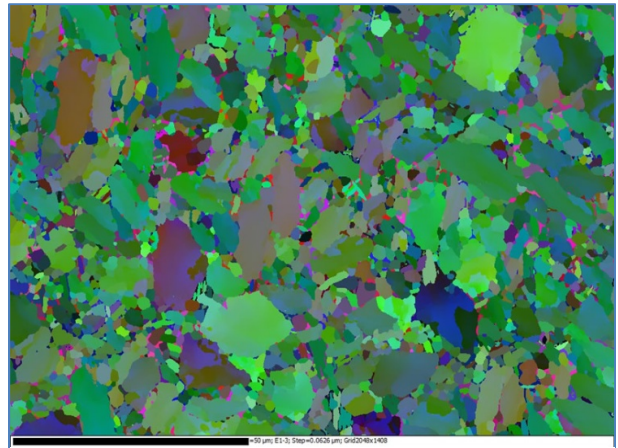


Figure 8: An example a grain size and direction map using inverse pole figures.<sup>(14)</sup>

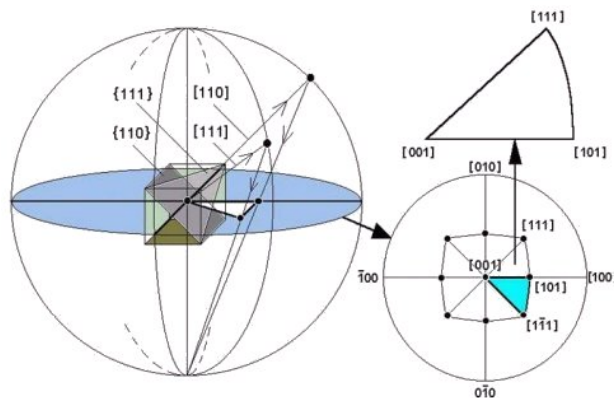


Figure 9: A figure demonstrating how orientation is captured by an inverse pole figure map with color coding.<sup>(14)</sup>

## Experimental Procedure

### Metallographic Preparation

A sample of forged René was sent from Carlton Forge Works to Cal Poly to be analyzed using optical microscopy techniques. Six sections were cut from the cross section and were carefully cataloged regarding their original location in the cross section (Figure 10). This was done to in an attempt to track the distribution of both large grains and discontinuous boundaries across the sample. Sections were chosen at the outer and inner edges as well as the top and bottom of the forging. Three samples were mounted in mineral filled diallyl phthalate (Bakelite) for better etching and edge retention for metallographic purposes and three samples were mounted in conductive Bakelite in order to minimize the effect of charge build up during scanning electron microscopy. All samples were prepared with first with sand paper to eliminate large defects. Then they were polished with a 6  $\mu\text{m}$  colloidal silica solution on a polishing wheel to take out the majority of the scratches from the sand paper. Finally, a 1  $\mu\text{m}$  colloidal silica solution was used to complete a final polish. These samples were then etched by submerging the sample in a solution of 95% hydrochloric acid and 5% hydrogen peroxide. The samples with conductive Bakelite were more difficult to etch due to the metals present in the Bakelite being more reactive than the Rene 41 metal itself, thus decreasing the effect of the etch and requiring more time for etching.

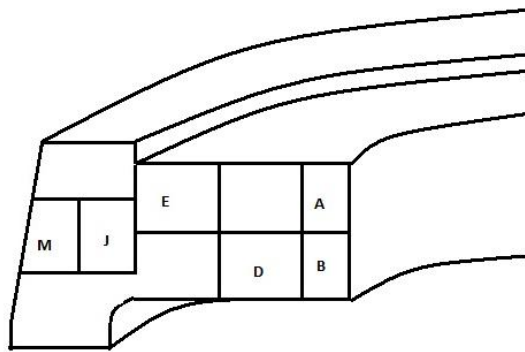


Figure 10: A schematic of the cross section detailing where samples originated from.



## Metallographic Grain Size Measurement

### Measuring Fine Grains

Grain sizing was established by taking five micrographs of the fine structure and one micrograph of the largest structure on the sample (ALA). The fine microstructure was measured using a computer aided overlay which measured average grain size following ASTM standard E112-96<sup>(15)</sup> (Figure 11). Fine grain regions in samples D, E, J, and M were measured five times to give an overall average fine grain size for each sample. The computer proved to be unreliable in its own formulation of grain sizing so some manual work in choosing grain boundaries was done to calculate grain size.

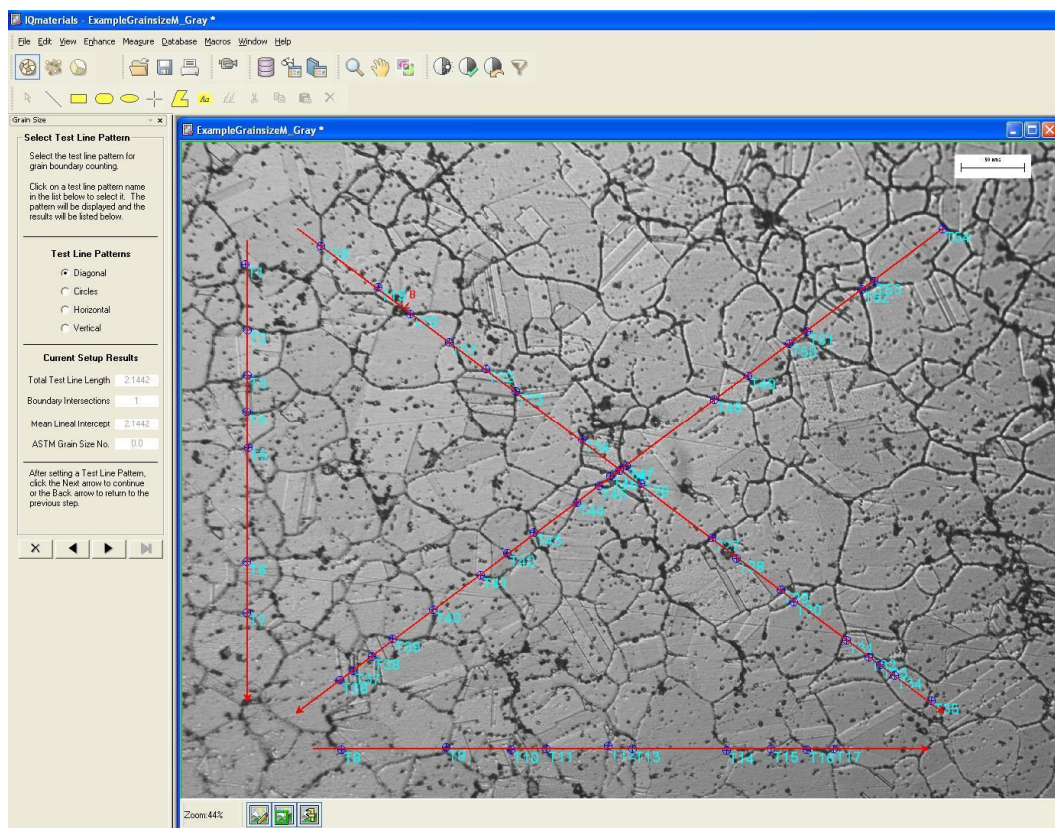


Figure 11: An example of how grain size was measured using a computer overlay of the diagonal measuring tool. Each of the blue marks indicates a manually marked grain boundary intersection.

### Estimation of Large Grain Sizes

ALA grain size was quantified by measuring the longest length of the grain and the widest perpendicular width. Those two measurements were multiplied together along with a factor that corrects for an elliptical shape as described by ASTM standard E930-99<sup>(16)</sup> (Figure 12). Estimating the percent area covered by large grains was done in accordance with figures in ASTM standard E1181-02<sup>(17)</sup> (Figure 13). Choosing whether to count the discontinuous grains as part of grain size was a difficult choice; however they were not included because of their lack of continuity. The definition of a grain boundary is defined as the internal interfaces that separate two misoriented single crystals in a polycrystalline solid.<sup>(11)</sup> If their boundary cannot complete a closed loop, then it was assumed that their grains are the same orientation. Even though this problem is at the heart of the project, the grains would initially be counted by standard procedures outlined by ASTM standards E1181-02 and E930-99.

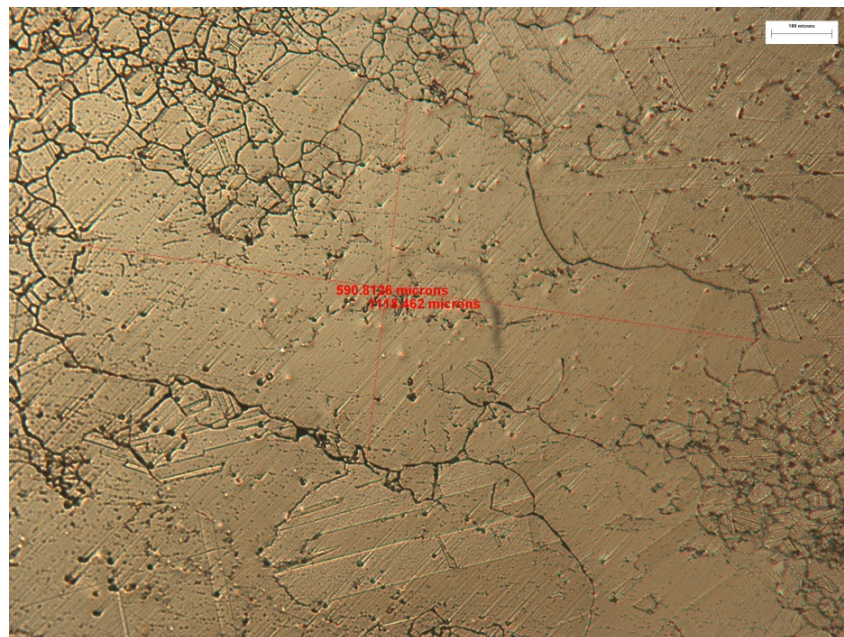


Figure 12: A micrograph describing the technique used for measuring the largest grain (ALA) of a sample.

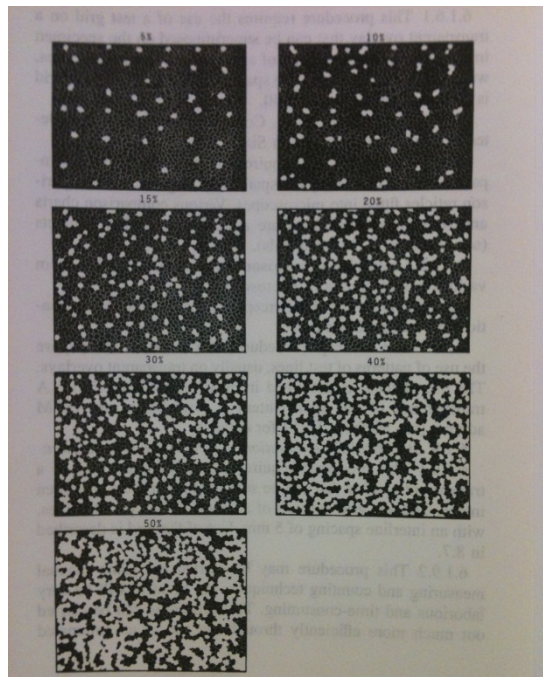


Figure 13: An excerpt from ASTM standard 1181-02 comparison chart of relative percentages of duplex grain size.<sup>(17)</sup>

### SEM-EBSD Preparation

Sample preparation is a critical step for EBSD because of the surface-sensitive nature of the analysis.

Electrons beamed at the sample surface only penetrate a few nanometers; therefore any surface defects can cause the image to become blurred. Sample J was sent to Evans Analytical Group (EAG) for SEM-EBSD analysis and was remounted in a nickel-epoxy matrix. The nickel-epoxy matrix is conductive to allow any charge buildup due to electrons incident on the surface. The sample was then sanded with 1200 grit silicon carbide paper for 1 minute with an automated polishing wheel to remove contaminants and any large surface defects. The sample was then polished with a synthetic rayon cloth and a 1  $\mu\text{m}$  alumina suspension for 10 minutes. After a quick rinse, the sample was polished on another synthetic rayon cloth and a 0.03  $\mu\text{m}$  alumina suspension for 10 additional minutes.<sup>(18)</sup> The sample was then placed into the SEM at EAG for EBSD analysis.



## Results

### Fine Grain Sizes

The fine grain structures had few discontinuous grains among them and were relatively easy to quantify grain size (Figure 14). The fine grains were consistently found to be ASTM grain size 5 to 7 in size across the cross section with a pooled standard deviation of 0.357 (Figure 15). Samples A and B had mostly coarse grains with a few bands of fine grains and were more difficult to rate (Figure 16). Consequently both regions were rated to a wide range condition of having grains as small as ASTM 5 and as large as ASTM -1. The mean grain size for samples A and B were ASTM 4.70 and ASTM 3.87 respectively.

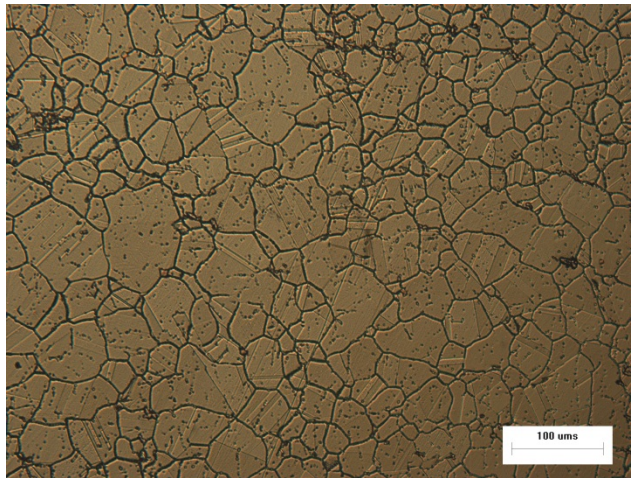


Figure 14: A typical microstructure of fine grains at 200X found near the outer edge of the part in sample M.

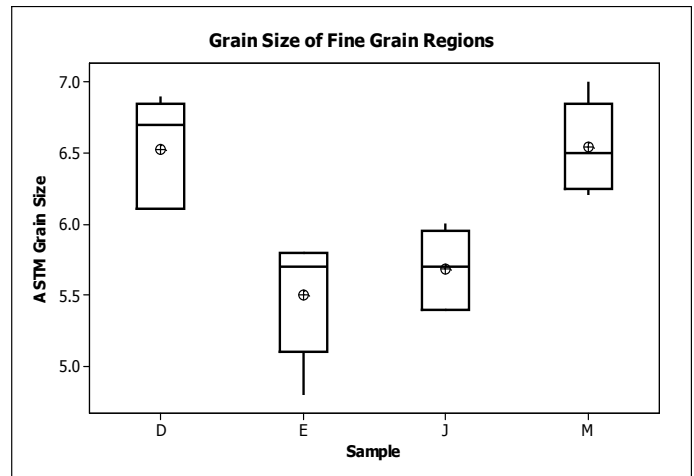


Figure 15: A box plot of average fine grain sizes in samples D, E, J, and M with a pooled standard deviation of 0.357.

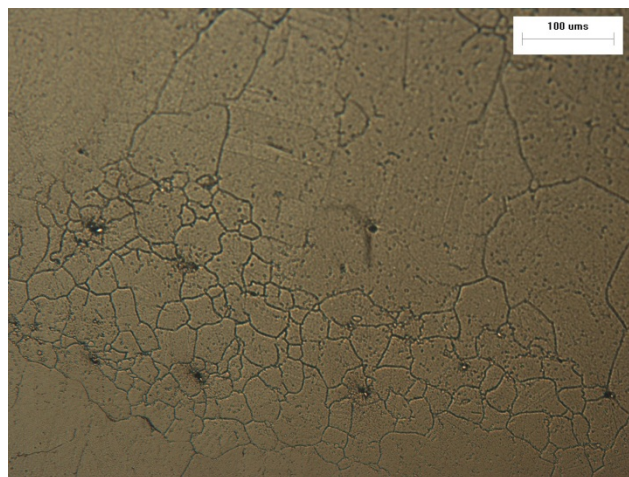


Figure 14: Sample A showing a small band of fine grains in amongst much coarser grains.

## Coarse Grain Sizes

Coarse grains were typically found to be ASTM 2 to 1 with an as large as (ALA) grain size of -1. The presence of twinning boundaries running across the majority of the coarse grain indicated that these grains are in fact significantly larger than the fine grains (Figure 17). Twinning boundaries by definition extend from grain boundary to grain boundary in a linear fashion due to stacking faults in the lattice.<sup>(11)</sup> Thus, no grain boundary can exist across a twinning boundary. This is conclusive proof that the large majority of these grains are coarse and single crystalline. The etchant is not attacking the twinning boundaries themselves, only the difference in orientation of the lattice caused by the stacking fault causes the area to etch slightly differently. However, this does not prove that the grains are entirely homogeneous; there still is some evidence of discontinuous grains that do not violate the twinning boundary.

The abundance of these coarse grains changes dramatically across the cross section (Figure 18). Moving from the outer diameter to the inner diameter of the forged ring, the presence of fine grains significantly diminishes.

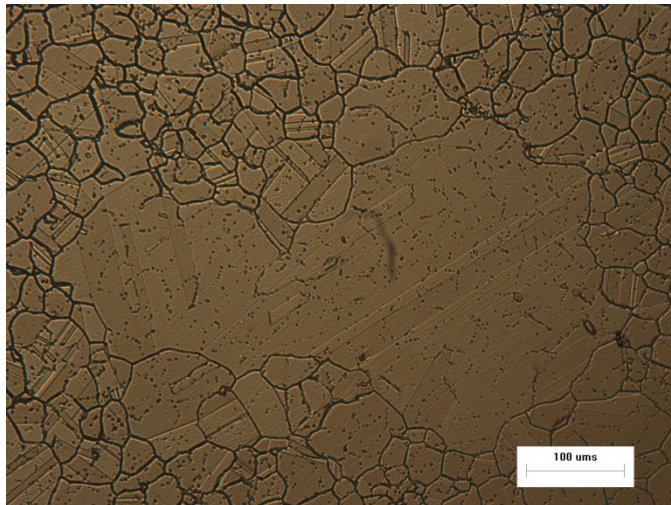


Figure 16: A purposefully over etched sample of a typical large grain seen with twinning boundaries running across.

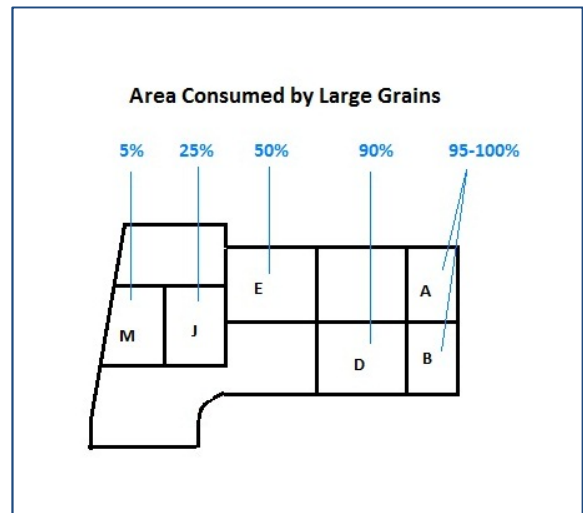


Figure 17: Distribution of large grains across the cross section.

## Optical Verification of Discontinuous Grains

Upon closer examination, it appeared that the grain boundaries were not simply a precipitate that formed an incoherent line (Figure 19). Twinning boundaries also seemed to start or end at them indicating that they probably are grain boundaries. However, etching times really didn't improve the continuity of the grain boundaries in question. Other grain boundaries widened and other areas burned to the point of making grain sizing for the rest of the sample very difficult before any of these discontinuous grain boundaries would become observable and coherent boundaries. As a result EBSD would have to be done to conclusively determine the polycrystalline grain structure of the forged René 41.

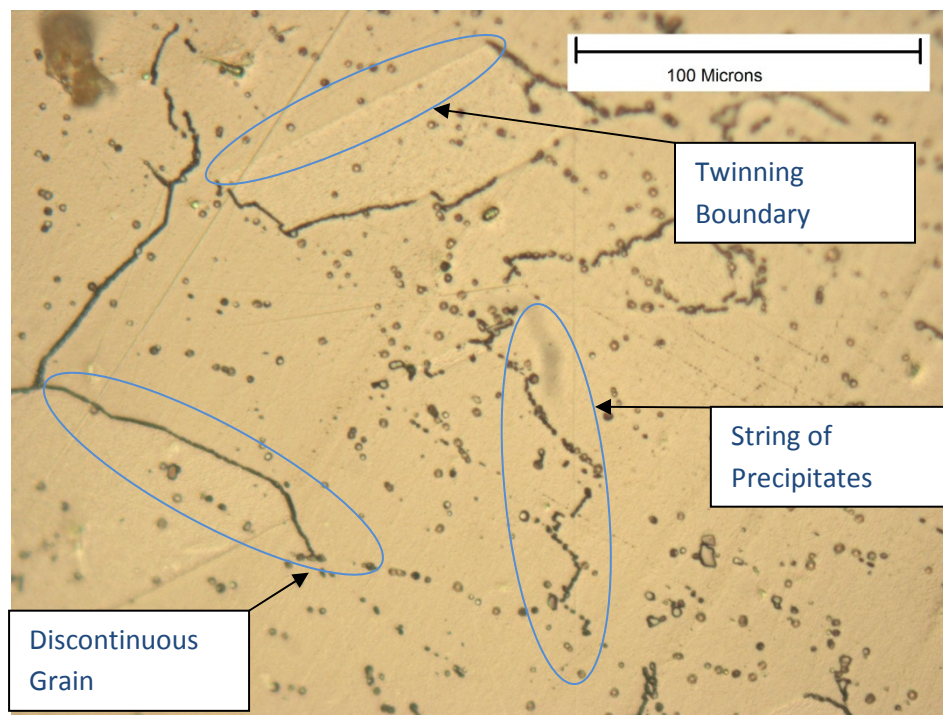


Figure 18: A micrograph of a discontinuous grain taken at 500x where there is a clear distinction between twinning boundaries, precipitates, and discontinuous grain boundaries



## SEM-EBSD

### Image Quality Map

An image quality map of sample J shows an area with few precipitates and primarily large grains with a few finer grains on the right-hand side of the image (Figure 20). An overlay of possible twinning boundaries was done to illustrate the location and relative boundary angle (Figure 21). Red boundaries indicate a boundary angle of  $58^{\circ}$  to  $62^{\circ}$  while green boundaries indicate a boundary angle of  $37^{\circ}$  to  $41^{\circ}$ . Notice how the majority of the grains outlined in the red are twinning boundaries due to their linear fashion. However, most of the green grain boundaries follow what looks like grain boundaries because of their non-linear shape. Also to be noted is the significantly diminished amount of low angle boundaries in the fine grain areas while the area with coarser grains appears to be more abundant with low angle boundaries.

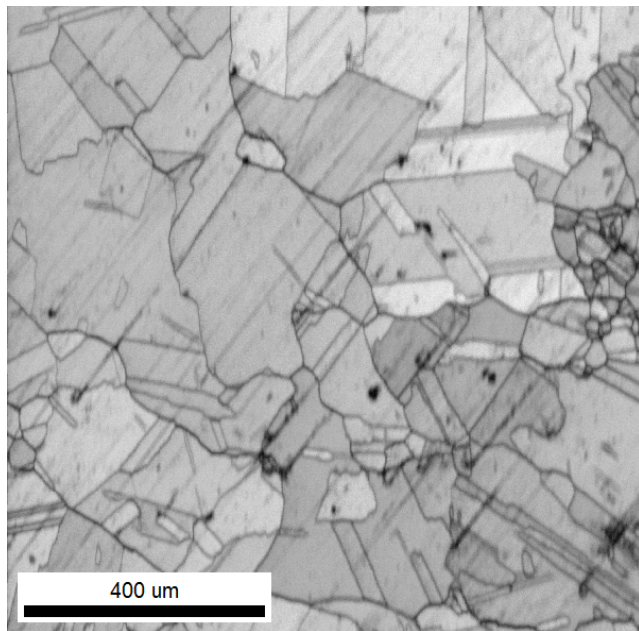


Figure 20: An image quality map, produced by EBSD, shows the majority of the area being consumed by large grains.

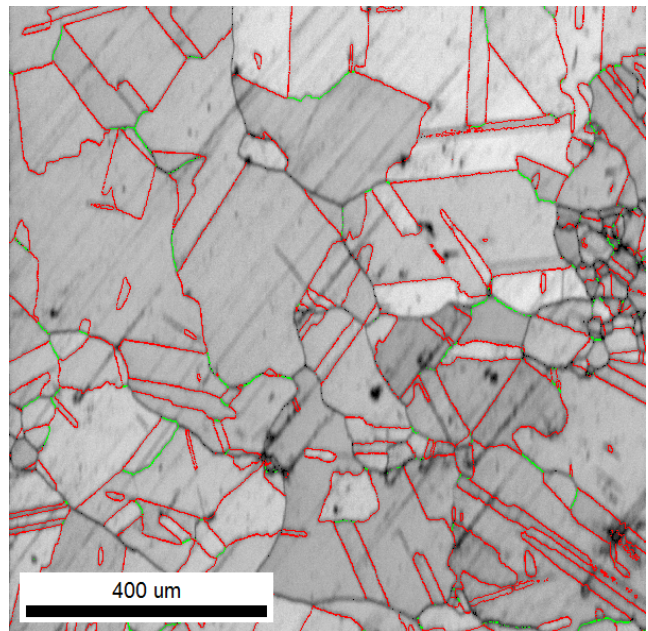


Figure 19: An overlay of possible low angle boundaries over the original image quality map of figure 20. Red and Green lines illustrate low angle grain boundaries; however green lines are lower angle than red.

## Inverse Pole Figure

An inverse pole figure was compiled to illustrate the orientation of each grain relative to one another (Figure 22 and 23). This allows us to characterize why some boundaries are not apparent in during optical microscopy. Regions that are similar in color reflect similar orientation. Most grains do not lie precisely on the real world vectors  $[001]$ ,  $[101]$ , and  $[111]$ ; so most crystal structures are a shade of in between those vectors.

To illustrate the existence of low angle grain boundaries, take note of the large yellow grain in the upper left region of the orientation map. That region is clearly all very similar in orientation. However according to the image quality map in figures 20 and 21, the same yellow region is broken up into two grains separated by a low angle grain boundary outlined in green.

Color Coded Map Type: Inverse Pole Figure [001]  
Nickel

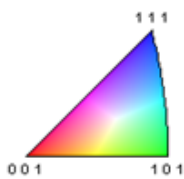


Figure 22: A color map type describing how the real world vectors  $[001]$ ,  $[101]$ , and  $[111]$  correlate to the colors red, green, and blue respectively.

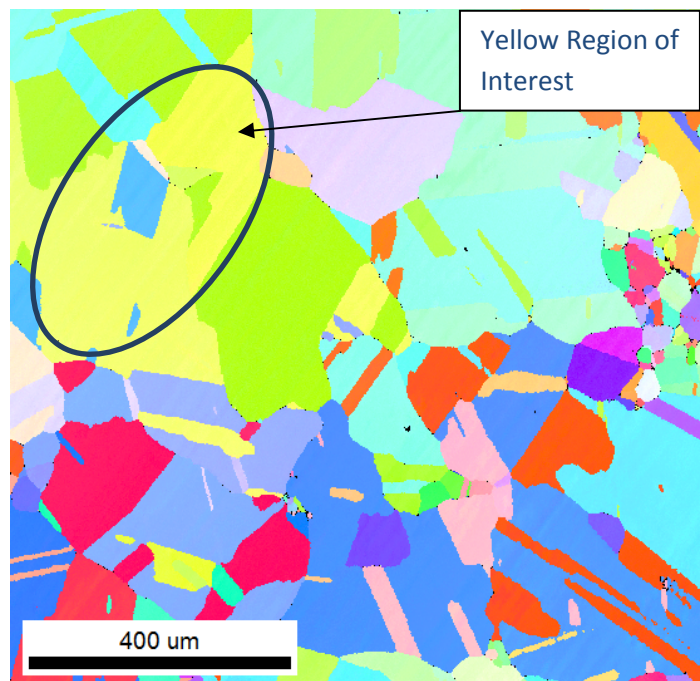


Figure 21: An inverse pole figure relating a specific color to a particular crystallographic orientation.

## Discussion

### Topological Duplex Grain

Discontinuous grains were only significant in coarse grains because of the difficulty in rating these grains, so there is an importance of tracking the occurrence of these coarse grains and identifying what is causing them to occur. The grain structure found on the part can be characterized as a topological duplex grain sizing. This is where there are two or more grain sizes whose distribution changes depending on where on the part the observer is looking. As a result, it is important to note that large grains only began to appear in large amounts towards the inner diameter of the part.

This can be attributed to a difference in strain across the part. The inner diameter may not be receiving the amount of strain required for dislocations to pin down grain boundaries. Therefore during recrystallization, grains are more favorable to expand and consume other grains rather than nucleate many finer grains that limit growth. It is evident that the crystal structure is fully recrystallized so there was enough work done to cause grains to recrystallize in order to release residual stress in the microstructure of higher energy grains.

### Correlation between Discontinuous and Low Angle Grain Boundaries

Based on the EBSD results from both the inverse pole figure and image quality map, we can conclude that low angle grain boundaries exist to a great extent in the large grains of René 41. These low angle grain boundaries have lower surface energies associated due to the cohesion between the two lattices. Corrosive agents are less likely to attack low surface energy boundaries when there are other higher surface energy grain boundaries present. As such, the discontinuous grains could be attributed to this phenomenon based on the idea that low angle grain boundaries have lower surface energy and are less likely to be attacked by corrosive agents.

## Recommendation for Further Study

It is unclear how these low angle grain boundaries might affect material properties of forged René 41. They may enhance the properties as some research suggests that these grain boundaries in IN718 help to inhibit oxygen induced intergranular fracture at elevated temperatures.<sup>(19)</sup> A conclusive way to determine if low angle grain boundaries have the same mechanical ability would be to purposefully create two samples with similar grain size but one would contain lower angle grain boundaries. These two samples could be mechanically tested in a number of ways including: tensile strength at room temperature and elevated temperatures, stress rupture testing with and without notches, fatigue life in both low cycle and high cycle, and creep. Because low angle grain boundaries appear more frequently in larger grains, both samples would have to be of fairly large grains. However, careful characterization of the grain boundaries would be required both optically and using the SEM-EBSD to coincide with the mechanical strength characterization.

## Conclusions

1. Discontinuous grain boundaries were most prevalent in large grains, which lead to discrepancies in what grain size they follow.
2. Large grains were found to be located more predominantly in the inner diameter of the forged ring.
3. Discontinuous grains were found to be continuous grains with coincident site lattice boundaries which are resistant to chemical attack.

## References

1. **Reed, Roger C.** *The Superalloys: Fundamentals and Applications*. Cambridge : Cambridge University Press, 2006.
2. **Klopp, William D.** Rene 41. *Aerospace Structural Metals Handbook*. West Lafayette, IN : Purdue Research Foundation, 1994, p. Code 4205.
3. F-16 Design & Construction. [Online] February 1, 2007. [Cited: January 19, 2012.] [http://www.f-16.net/f-16\\_forum\\_viewtopic-t-840.html](http://www.f-16.net/f-16_forum_viewtopic-t-840.html).
4. ABET Criteria for Accrediting Engineering Programs 2010-13, General Criteria for Baccalaureate Level Programs, General Criteria 3: Student Outcomes. [Online] <http://www.abet.org/engineering-criteria-2012-2013/>.
5. **Bowman, Randy.** Superalloys: A Primer and History. *TMS*. [Online] [Cited: April 9, 2012.] <<http://www.tms.org/Meetings/Specialty/Superalloys2000/SuperalloysHistory.html>>.
6. **Trupo, Mary.** Aerospace Industry Is Critical Contributor to U.S. Economy According to Obama Trade Official at Paris Air Show. *Department of Commerce - United States of America*. [Online] June 21, 2009. [Cited: April 9, 2012.] <http://trade.gov/press/press-releases/2011/aerospace-industry-critical-contributor-to-us-economy-062111.asp>.
7. **Sangid, Michael D., et al., et al.** Grain boundary characterization and energetics of superalloys. Urbana, IL : Materials Science and Engineering A, 2010, pp. 7115-7125.
8. Ring Rolling. *Forging-Industry*. [Online] SK Forging. [http://www.forging-industry.com/bearing\\_manufacturer.asp?aid=17](http://www.forging-industry.com/bearing_manufacturer.asp?aid=17).
9. **Hayes, Robert and Combs, Steve.** *Metals Technology Inc. Discontinuous Grains Discussion*. Northridge, CA, April 19, 2012.
10. **Decker, Raymond Frank, et al., et al.** *Abnormal grain growth in nickel-base heat-resistant alloys*. Ann Arbor, Michigan : University of Michigan: Engineering Research Institute, 1956. Report 51 to National Advisory Committee for Aeronautics.
11. **Abbaschian, Reza, Abbaschian, Lara and Reed-Hill, Robert E.** *Physical Metallurgy Principles*. Stamford, CT : Cengage Learning, 1994.
12. *Applications for Grain Boundary Engineered Materials*. **Palumbo, G., Lehockey, E.M. and Lin, P.** 1998, JOM, pp. 40-43.
13. *The effect of grain-boundary-engineering-type processing on oxygen-induced cracking of IN718*. **Krupp, Ulrich, et al., et al.** 2002, Materials Science and Engineering: A, pp. 214-217.
14. EBSD Electron Backscatter Diffraction Analysis. [Online] 2011. [Cited: February 1, 2012.] <http://www.ebsd.com/>.



15. Standard Test Methods for Determining Average Grain Size. *ASTM Standards: Metals Test Methods and Analytical Procedure*. West Conshohoken, PA : ASTM International, 2004. Vol. 03.01. E112-96.
16. Standard Test Methods for Estimating the Largest Grain Size Observed in a Metallographic Section (ALA) Grain Size. *ASTM Standards: Metals Test Methods and Analytical Procedure*. West Conshohoken, PA : ASTM International, 2004. Vol. 03.01. E930-99.
17. Standard Test Methods for Characterizing Duplex Grain Sizes. *ASTM Standards: Metals Test Methods and Analytical Procedure*. West Conshohoken, PA : ASTM International, 2004. Vol. 03.01. E1181-02.
18. *EDAX Launches the New TEAM™ Pegasus Analysis System*. **Coy, Mike, et al., et al.** 1, s.l. : EDAX Inc., 2012, Vol. 10.
19. *Brittle intergranular fracture of a Ni-base superalloy at high temperatures by dynamic embrittlement*. **Krupp, U., et al., et al.** 2003, Materials Science and Engineering: A, pp. 409-413.

## Acknowledgements

There were many individuals who assisted me during my journey to complete my project. Firstly, I would like to thank Bob Keener at Carlton Forge Works for sponsoring the project and for considerable help in understanding the background of the project. I would also like to thank Steve Combs and Bob Hayes of Metals Technology Inc. who were instrumental in a number of ways. Steve assisted in proper etching and rating techniques used by industry professionals. Bob Hayes helped me understand the fundamentals of special coincident site lattices and for that I cannot thank them enough. Finally, I would like to thank my advisor, Prof. Blair London, for keeping me on track and giving guidance to accomplish my goal.